J|A|C|S
ARTICLES
Published on Web 01/22/2002

Nucleation and Growth of Germanium Nanowires Seeded by Organic Monolayer-Coated Gold Nanocrystals

Tobias Hanrath and Brian A. Korgel*

Contribution from the Department of Chemical Engineering, Texas Materials Institute, Center for Nano- and Molecular Science and Technology, The University of Texas at Austin, Austin, Texas 78712-1062

Received August 7, 2001

Abstract: Germanium nanowires, ranging from 10 to 150 nm in diameter, were grown several micrometers in length in cyclohexane heated and pressurized above its critical point. Alkanethiol-protected gold nanocrystals, either 2.5 or 6.5 nm in diameter, were used to seed wire formation. Growth proceeded through a solution−liquid−solid mechanism at growth temperatures ranging from 300 to 450 °C. At temperatures exceeding 500 °C, large Ge particulates formed due to unfavorable growth kinetics. Temperature, the nature of the precursor, precursor concentration, and the Au:Ge ratio were determining factors in nanowire morphology. The Ge nanowires were characterized using a range of techniques, including XPS, XRD, high-resolution TEM and SEM, nanometer-scale EDS mapping, and DTA.

Introduction

Semiconductor nanowires have recently been under intense investigation, encouraged by new synthetic methods and their potential use in applications ranging from integrated circuit interconnects to functional electronic and optical devices.[1−4] In addition to significant technological advances due to their unique electrical, optical, and mechanical properties, nanowires can provide a material system to experimentally test fundamental quantum mechanical concepts.

For many applications, nanowires must be crystalline and largely defect-free, with diameters ranging from 10 to 100 nm and lengths greatly exceeding their diameter. Remarkable new synthetic methods have produced nanometer diameter wires with aspect ratios greater than 1000 for a variety of semiconducting materials, such as silicon,[5−7] germanium,[5,8−12] and GaAs.[1,13] Compared to Si, Ge nanostructures are of particular interest, since the Bohr exciton radius is larger in Ge than in Si,[14] which consequently should lead to more prominent quantum confinement effects. Herein, we report the solution-phase synthesis of Ge nanowires ranging from 10 to 150 nm in diameter with lengths up to several micrometers.

The approach described here is based on the vapor−liquid−solid (VLS) whisker growth mechanism discovered by Wagner and Ellis[15,16] over 30 years ago. In the first VLS experiments, a silicon precursor was degraded from the gas phase by chemical vapor deposition (CVD) over a surface containing liquid gold droplets. Instead of depositing on the surface, the silicon preferentially dissolves into the gold droplet to form a Au:Si alloy until saturation. Upon saturation, the semiconductor exits the droplet in the form of a whisker (see Scheme 1). Growth is sustained by continued Si absorption into the nucleating metal drop as the CVD reaction proceeds. Since this method was originally applied with liquid metal drops, the minimum wire diameter achievable was limited to the minimum stable liquid drop diameter (i.e., ∼100 nm) and was limited to growth on a surface by vapor deposition.

As mentioned above, the VLS method has since been extended to a variety of materials[1,5−13] and modified to include a solution−liquid−solid (SLS) synthesis,[17] gas-phase synthesis with nucleation particles created via laser ablation,[5] and a supercritical fluid synthesis.[18] The laser ablation method has been successfully applied to various semiconductor materials such as Si, Ge, GaN, and GaAs,[1,5,19] although the wire diameters have had large size distributions. Naturally, one expects to have better diameter control by controlling the size of the nucleating

* Corresponding author. Phone: (512) 471-5633. Fax: (512) 471-7060. E-mail: korgel@mail.che.utexas.edu.

(1) Hu, J.; Odom, T. W.; Lieber, C. M. *Acc. Chem. Res.* **1999**, *32*, 435.
(2) Prokes, S. M.; Wang, K. L. *Mater. Res. Sci. Bull.* **1999**, *24*, 13.
(3) Duan, X.; Huang, Y.; Cui, Y.; Wang, J.; Lieber, C. M. *Nature* **2001**, *409*, 66.
(4) Cui, Y.; Lieber, C. M. *Science* **2001**, *291*, 851.
(5) Morales, A. M.; Lieber, C. M. *Science* **1998**, *279*, 208.
(6) Wang, N.; Tang, Y. H.; Zhang, Y. F.; Lee, C. S.; Lee, S. T. *Phys. Rev. B* **1998**, *58*, R16024.
(7) Coleman, N. R. B.; Morris, M. A.; Spalding, T. R.; Holmes, J. D. *J. Am. Chem. Soc.* **2001**, *123*, 187.
(8) Wu, Y.; Yang, P. *Chem. Mater.* **2000**, *12*, 605.
(9) Zhang, Y. F.; Tang, Y. H.; Wang, N.; Lee, C. S.; Bello, I.; Lee, S. T. *Phys. Rev. B* **2000**, *61*, 4518.
(10) Omi, H.; Ogino, T. *Appl. Phys. Lett.* **1997**, *71*, 2163.
(11) Coleman, N. R. B.; Ryan, K. M.; Spalding, T. R.; Holmes, J. D.; Morris, M. A. *Chem. Phys. Lett.* **2001**, *343*, 1.
(12) Heath, J. R.; LeGoues, F. K. *Chem. Phys. Lett.* **1993**, *208*, 263.
(13) Shi, W.; Zheng, Y.; Wang, N.; Lee, C. S.; Lee, S. T. *Adv. Mater.* **2001**, *13*, 591.
(14) Maeda, Y.; Tsukamoto, N.; Yazawa, Y.; Kanemitsu, Y.; Masumoto, Y. *Appl. Phys. Lett.* **1991**, *59*, 3168.
(15) Wagner, R. S.; Ellis, W. C.; Jackson, K. A.; Arnold, S. M. *J. Appl. Phys.* **1964**, *35*, 2993.
(16) Wagner, R. S.; Ellis, W. C. *Appl. Phys. Lett.* **1964**, *4*, 89.
(17) Trentler, T. J.; Hickman, K. M.; Goel, S. C.; Viano, A. M.; Gibbons, P. C.; Buhro, W. E. *Science* **1995**, *270*, 1791.
(18) Holmes, J. D.; Johnston, K. P.; Doty, R. C.; Korgel, B. A. *Science* **2000**, *287*, 1471.
(19) Duan, X.; Lieber, C. M. *J. Am. Chem. Soc.* **2000**, *122*, 188.

10.1021/ja016788i CCC: $22.00

Scheme 1. Binary Phase Diagram for the Au:Ge (Adapted from Ref 22)[a]

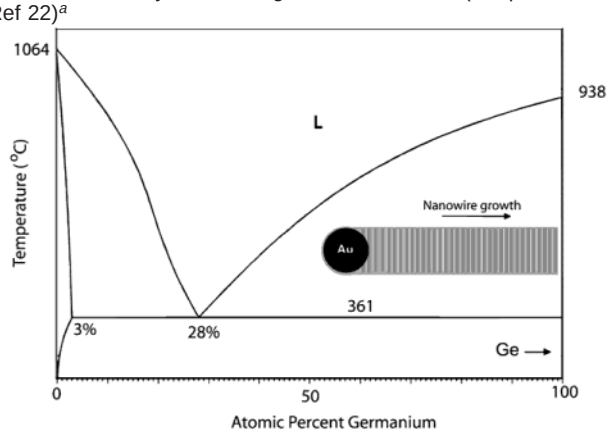

[a] The inset illustrates the proposed nanowire growth mechanism. The germanium precursor thermolytically degrades to atomic Ge, which dissolves in Au seed particles. Upon saturation, Ge crystallizes in the form of single-crystal wire.

metal particles. Recently, we demonstrated that alkanethiol-protected gold nanocrystals dispersed in a supercritical fluid at high temperature and high pressure could indeed control Si nanowire growth to produce nanowires less than 10 nm in diameter, with relatively narrow size distributions.[18] Lieber and co-workers later reported diameter control of Si and InP nanowires by combining CVD with size-monodisperse Au particles ranging in size from 5 to 30 nm attached to a surface.[20,21] In a fluid, the dispersed Au nanocrystals can produce free-floating nanowires with dramatically higher throughput than surface growth methods. The solution-phase approach affords rational tunability of the synthesis parameters, such as precursor and seed concentration and size, while providing a high-temperature and high-diffusion-rate environment for the reaction.

Binary metal phase diagrams provide a general guide for selecting suitable materials to seed wire growth. The bulk phase diagram for Au:Ge shown in Scheme 1 reveals the coexistence of a liquid solution with solid Ge above the eutectic point at 28 at. % Ge and a temperature of 360 °C.[22] Wu and Yang recently presented unambiguous evidence for the VLS mechanism in Au-nucleated Ge nanowires.[23] Herein, we report the solution-phase synthesis of Ge nanowires using alkanethiol-capped Au nanocrystals, dispersed in cyclohexane heated and pressurized above its critical point, as the seeds for wire growth. The effects of temperature, pressure, precursor, reaction time, and precursor concentration were investigated. The optimum conditions for Ge nanowire growth are identified.

Experimental Section

Nanowire Formation. The experimental setup was similar to one applied by Chlistunoff et al.[24] A modification was made to create a flow-through reactor that permitted rapid thermal quenching after the reaction and efficient product purification by flushing the reactor with cyclohexane (Figure 1). The inlet and outlet of a 1.6-mL grade 2 titanium reaction cell were connected to high-pressure tubing via LM-6

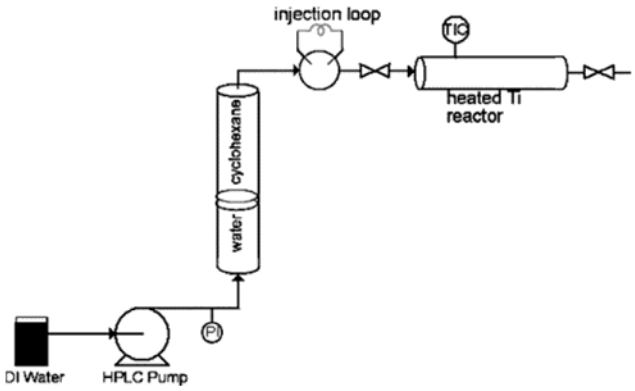

Figure 1. Apparatus for nanowire synthesis in supercritical fluid.

HIP reducers (High-Pressure Equipment Co.). A Si (100) wafer was placed inside the reactor cell to help collect the nanowires after the reaction. The deposition wafers were cut into 4- × 30-mm sections and sonically cleaned in acetone for 40 min, followed by a rinse in 2-propanol and a 15-min rinse in a 1:1 HCl:methanol solution. They were then rinsed and stored in doubly distilled, deionized water prior to insertion into the reactor. The cell was covered with heating tape (Barnstead/Thermolyne) and insulation, allowing the reactor temperature to be maintained to within ±1 °C through a temperature controller (Omega). A high-pressure liquid chromatography (HPLC) pump (Alcott) was used to pressurize a piston with doubly distilled, deionized water which in turn pressurized the reactor with deoxygenated, anhydrous cyclohexane (Aldrich). The system pressure was monitored with a digital pressure gauge (Sensotech).

Alkanethiol-coated Au nanocrystals were prepared and size-selected according to procedures outlined in the literature.[25,26] The germanium precursors were tetraethylgermane (TEG; $(CH_3CH_2)_4Ge$, Aldrich, 99%) and diphenylgermane (DPG, $(C_6H_5)_2H_2Ge$, Gelest, 95%). A stock solution of Au nanocrystals in the germanium precursor (Au:Ge molar ratio 1:2000) was prepared under a nitrogen atmosphere. The nanocrystals/Ge precursor stock solution was diluted in anhydrous deoxygenated cyclohexane to 200 mM Ge and used as the injection solution. Several reactor volumes of anhydrous deoxygenated cyclohexane were flushed through the cell prior to precursor injection to ensure an oxygen-free synthesis environment. The titanium cell was pressurized with cyclohexane to 2.0 MPa and heated to the desired synthesis temperature. Prior to precursor injection, the cell pressure was reduced from 7.6 to 4.2 MPa. The precursor solution was injected through a 350-μL sample loop into the supercritical cyclohexane in the hot reactor. The reactor was subsequently pressurized to the desired conditions, and the reaction proceeded for 8 or 20 min. After the elapsed synthesis time, the heating tape and insulation were removed. The cell was depressurized by ejecting the liquid reaction mixture into a receiving vial containing cyclohexane. The remaining products were extracted by flushing the reactor with cyclohexane, which also cleaned the nanowires deposited on the wafer. Water was sprayed on the cell to further decrease the reactor temperature. Any remaining products were isolated from the reactor by flushing with cyclohexane. The product solutions and the deposition wafer were stored under nitrogen prior to characterization. The achieved yields ranged from 60% to 80%.

Characterization. The Ge nanowires were characterized using various techniques. High-resolution scanning electron microscopy (HRSEM) was performed using either a Hitachi S-4500 or a LEO 1530, both operating at 10kV. Nanometer-scale energy-dispersive X-ray energy spectral (EDS, iXRF Systems, Inc.) maps were obtained on the LEO 1530 HRSEM with 6 kV accelerating voltage. The lateral pixel resolution was 128, with a pixel dwell time of 130 μs and a minimum

(20) Cui, Y.; Lauhon, J.; Gudiksen, M. S.; Wang, J.; Lieber, C. M. *Appl. Phys. Lett.* **2001**, *78*, 2214.
(21) Gudiksen, M. S.; Wang, J.; Lieber, C. M. *J. Phys. Chem. B* **2001**, *105*, 4062.
(22) *Binary Alloy Phase Diagrams*, 2nd ed.; ASM International: Materials Park, OH, 1990; Vol. 1.
(23) Wu, Y.; Yang, P. *J. Am. Chem. Soc.* **2001**, *123*, 3165.
(24) Chlistunoff, J.; Ziegler, K. J.; Lasdon, L.; Johnston, K. P. *J. Phys. Chem. A* **1999**, *103*, 1678.
(25) Brust, M.; Walker, M.; Bethell, D.; Schiffrin, D. J.; Whyman, R. *J. Chem. Soc., Chem. Commun.* **1994**, *801*, 1994.
(26) Korgel, B. A.; Fitzmaurice, D. *Phys. Rev. Lett.* **1998**, *80*, 3531.

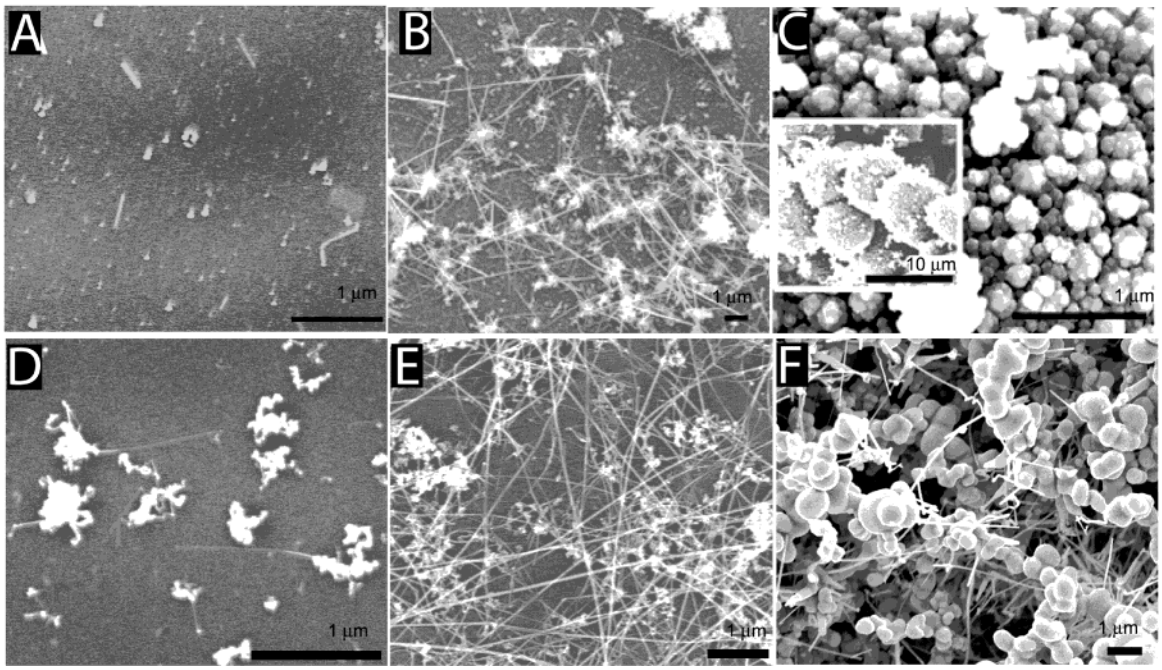

Figure 2. HRSEM images of Ge nanowires grown at 38 MPa for 20 min using TEG at (A) 300, (B) 400, (C) 500 °C. Ge nanowires grown at 38 MPa for 8 min using DPG at (D) 300, (E) 400, and (F) 500 °C. The micrometer-sized particles in (C) and (F) are Ge particles, as confirmed by nanometer-scale EDS mapping. The morphology of wires produced from DPG with 20-min reaction time was similar to the those shown in (D)−(F). The inset in (C) shows a low-magnification image of micrometer spheres formed at 500 °C.

of 30 overlaid frames. Ge was detected using the Ge Lα line at 1.188 keV; Au and oxygen were detected using the M and Kα lines at 2.121 and 0.525 keV, respectively. Nanometer-resolved elemental contrast images were also obtained using a Robinson backscattering electron detector (RBSD, ETP Semra Ltd.) attached to the LEO 1530 SEM. High-resolution transmission electron microscopy (HRTEM) images and selected area electron diffraction (SAED) patterns were obtained using a JEOL 2010 or a JEOL 2010F electron microscope operating at 200 kV. HRTEM samples were prepared by drop casting cyclohexane-dispersed nanowires on carbon-coated 200 mesh Cu grids (Electron Microscope Sciences). HRTEM was performed on nanowires removed from Si wafers by sonicating in minimal volumes of cyclohexane after the HRSEM characterization. X-ray photoelectron spectroscopy (XPS) was performed on a Physical Electronics XPS 5700 equipped with monochromatic an Al X-ray source (Al Kα, 1.4866 keV). X-ray diffraction (XRD) spectra were obtained on glass slides using a Phillips vertical scanning diffractometer, with Cu Kα radiation and a scintillation detector. Thermal analysis of the nanowires was performed on a Perkin-Elmer Series 7 differential thermal analyzer (DTA).

Results and Discussion

Figure 2 shows HRSEM images of Ge nanowires synthesized from TEG (Figure 2A−C) and DPG (Figure 2D−F) in cyclohexane at 38 MPa at temperatures varying from 300 to 500 °C.[27] Nanowire growth was seeded with 6.5- and 2.5-nm-diameter alkanethiol-capped Au nanocrystals for reactions using TEG and DPG, respectively.[28] Ge nanowire deposits observed on the wafers spanning the length of the "hot zone" of the reactor were homogeneous in concentration and size across the entire substrate, thus demonstrating that the reactor contents are well mixed in the cell during synthesis without appreciable temperature gradients.

Syntheses carried out at 250 °C with either TEG or DPG did not yield wires. Neither precursor decomposes significantly at this temperature. At 300 °C, limited precursor decomposition occurs (Figure 2A,D). A few short wires (average diameter of 45 and 19 nm for samples prepared from TEG and DPG, respectively) appear; however, the majority of the product is in the form of Ge particles. Nanometer-scale EDS mapping confirmed that the particulates in Figure 2A consist of Ge and not Au. At 400 °C, wire production improves significantly. Comparison of HRSEM images of wires formed using TEG and DPG, such as those shown in Figure 2B,E, reveal that DPG yields much higher quality Ge nanowires than TEG. DPG produces longer wires with minimal particle formation. Wires exceeding 20 μm in length are observed. The average wire diameter of the nanowires produced from TEG at 400 °C was 87 nm, while DPG under the same synthesis conditions yields nanowires with an average diameter of 17 nm. The relative standard deviations for the diameters produced from TEG and DPG were 36% and 26%, respectively. The statistical averages are based on analyzing more than 100 wires. The variation in nanowire diameter results in part from the nanocrystal size distribution, which commonly has a relative standard deviation of 15%. However, microscopic fluctuations in growth conditions can also lead to broadening of the histogram. The growth kinetics also dramatically impact wire morphology and size distributions as well (see discussion below), and nanowires produced from DPG are significantly smaller and more monodisperse than those formed under identical conditions from TEG.

Two primary factors appear to broaden the nanowire size distribution: (1) Au nanocrystal agglomeration and (2) unfavorable decomposition kinetics in the case of TEG. The injected precursor solution contains relatively size-monodisperse, steri-

(27) A similar sequence of experiments was carried out with both Ge precursors at a synthesis pressure of 13.8 MPa, but the gross morphology of the deposited material from this sequence of experiments did not differ significantly from the ones shown in Figure 2.

(28) Similar experiments using TEG were performed using size-monodisperse Au nanocrystals with an average diameter of 3.4 nm; however, the nanowire diameter distribution did not have a significant statistical difference from that of the wires grown from the larger Au nanocrystals.

cally stabilized Au nanocrystals; however, agglomeration of nanocrystals or liquid alloy Au:Ge droplets at elevated temperatures could be expected and would subsequently lead to broad Ge nanowire diameter distributions. A control experiment in which the Au nanoparticles were subjected to the synthesis conditions in the absence of germanium precursor showed significant nanoparticle agglomeration. In fact, it is quite remarkable that the nanocrystals are sufficiently stable to yield nanowire size distributions with standard deviations about the mean diameter less than ±30% when DPG is used as a precursor. The greatest contributor to size distribution broadening appears to be the wire growth kinetics. TEG gives rise to larger wires with very broad size distributions, while DPG produces smaller wires with relatively narrow size distributions. These differences stem from the different decomposition kinetics of each precursor. TEG appears to be more kinetically stable, as much less Ge product results from the low-temperature reactions than when DPG is used. DPG can form radicals stabilized by the two phenyl substituents, leading to an efficient disproportionation reaction and faster decomposition kinetics than TEG. Slow decomposition kinetics result in slow Ge supply to the seed particle, which is particularly crucial in the early stages of the wire formation process. Fast decomposition, such as in the case of DPG, leads to efficient saturation of the Au nanocrystals to initiate nanowire crystallization. The slower decomposition kinetics of TEG, on the other hand, allows more time to elapse before the nanocrystals are saturated enough to produce wires. Particle agglomeration can occur during this "lag time", which could explain the production of larger average wire diameters.

Nanowire synthesis was also attempted at 500 °C. HRSEM images of the resulting material are shown in Figure 2C,F for TEG and DPG, respectively. Instead of nanowires, micrometer-size spherical particles form. Nanoscale EDS mapping indicates that the particles are, indeed, composed of primarily Ge, and XRD revealed that the particulates consist largely of crystalline cubic Ge. One explanation for particle formation at 500 °C is that Ge nanowires form initially but subsequently melt into particulates. This hypothesis is based on the findings by Wu and Yang[29] that the Ge melting temperature is significantly depressed in nanowires—to temperatures as low as 600 °C for 20-nm-diameter wires. DTA scans of nanowires prepared from DPG at 350 °C, however, did not show any evidence of nanowire melting at 500 °C. Another explanation centers around the kinetic competition between wire growth and homogeneous Ge particle nucleation and growth. The precursor decomposes into Ge atoms that can either dissolve into the Au:Ge droplets and crystallize into nanowires, or homogeneously nucleate into spherical particles. At temperatures below 500 °C, Ge nucleation from the liquid Au:Ge seed particles is faster than homogeneous Ge particle nucleation. However, at 500 °C, nanowire growth cannot be sustained because the Ge supply rate to the system overwhelms the nanowire crystallization rate. When the Au:Ge ratio is increased to 1:20 instead of 1:2000, the seed particles can sustain nanowire growth to a degree, as shown in Figure 3A,B for DPG and TEG reactants, respectively; however, the inset in Figure 3A also shows that homogeneous nucleation of Ge on the nanowire surface remains a competing mechanism, which severely degrades the quality of the nanowires.

(29) Wu, Y.; Yang, P. *Adv. Mater.* **2001**, *13*, 520.

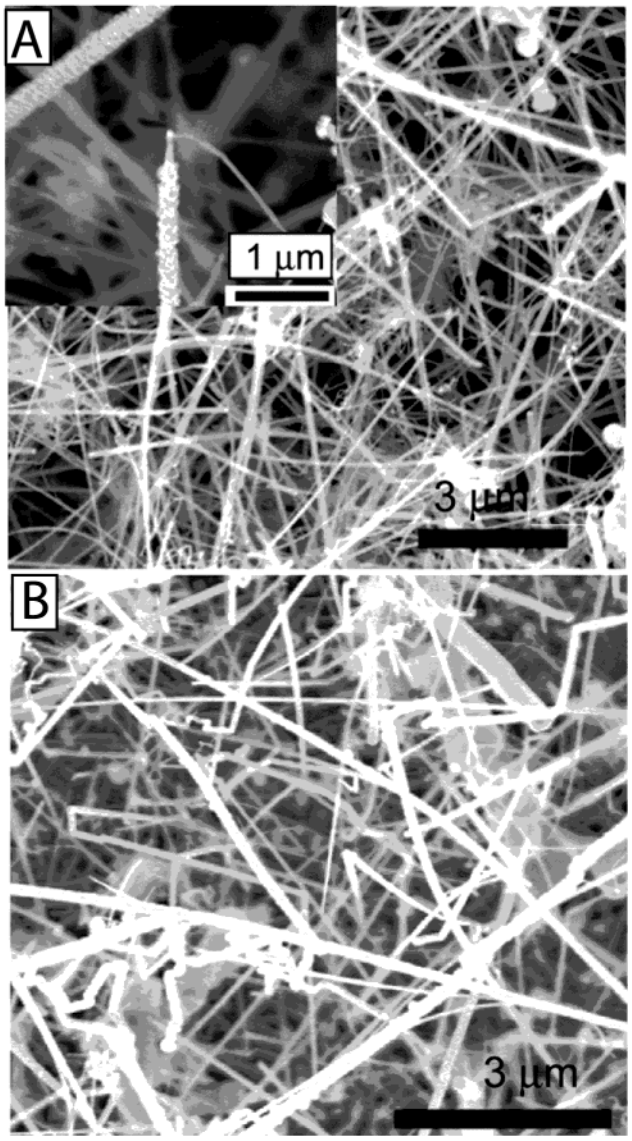

Figure 3. HRSEM images of Ge nanowires grown at 500 °C and 38 MPa with a Au:Ge ratio of 1:20 (A) using DPG and (B) using TEG. The inset in (A) shows the growth of excess Ge on the surface of the pre-existing nanowire.

The Ge nanowires synthesized in supercritical cyclohexane using gold nanocrystals as seeds exhibit crystalline cores. For example, HRTEM of Ge nanowires formed at 350 °C and 15 MPa using DPG exhibit cubic crystal structure, as shown in Figure 4A,B and confirmed by SAED (Figure 4A, inset) and XRD (Figure 4C). The HRTEM figures show that ⟨110⟩ and ⟨111⟩ are the predominant nanowire growth directions. A more detailed TEM study correlating the growth direction to synthesis parameters is currently in progress. Both SAED and XRD confirm that the Ge nanowire crystals have the cubic diamond structure. The Scherrer formula was used to estimate the effective domain size on the basis of fwhm of the diffraction peaks. The derived nanowire size produced from DPG at 400 °C was 20 nm, which agrees well with the 17 nm average wire diameter determined by TEM. Nanometer-scale EDS mapping of the Ge nanowires (Figure 5) confirms their Ge composition and also illustrates the presence of Au at the tips of the majority of the nanowires. Both nanometer-scale EDS maps and HRTEM confirm the direct participation of the Au nanocrystals in the

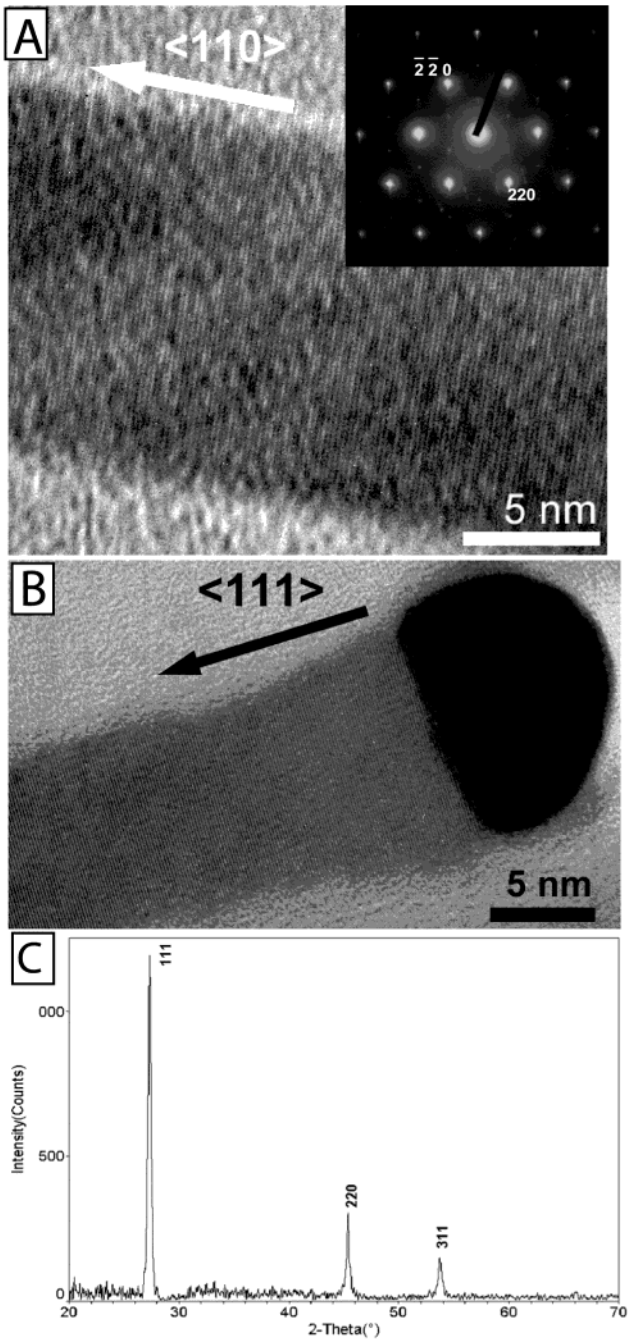

Figure 4. HRTEM and XRD of Ge nanowires (A) synthesized from DPG at 350 °C and 38 MPa, exhibiting the 110 growth direction, and (B) synthesized from TEG at 400 °C and 38 MPa, growing in the 111 direction. (C) XRD pattern of a nanowire sample obtained from DPG at 400 °C and 38 MPa. The inset shows the corresponding SAED pattern recorded along the [111] axis.

Ge nanowire growth. XPS (Figure 6) and EDS mapping (Figure 5) also show that, prior to atmospheric exposure, the Ge nanowires are not oxidized. After 24 h of atmospheric exposure, the wires oxidize to a significant degree, with 3 mol % O relative to Ge (Figure 5). After 168 h, approximately 7 mol % of the Ge in the sample has oxidized.

On the basis of the VLS and SLS mechanisms, one would not expect to form wires at temperatures below the eutectic temperature. However, Ge nanowires were observed to form at reaction temperatures as low as 300 °C. There are two possible explanations for this observation. Either the Au:Ge eutectic

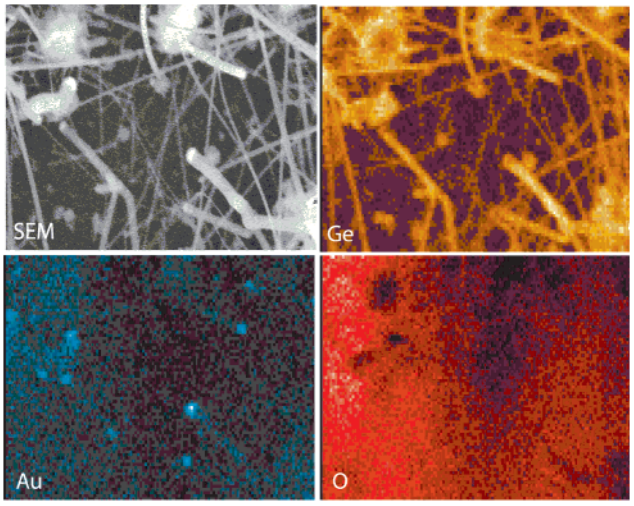

Figure 5. EDS map of Ge nanowires synthesized at 450 °C and 10 MPa showing Ge, Au, and O atomic profiles in the nanowires (Ge Kα, 1.188 eV; Au M, 2.121 eV; O Kα, 0.525 eV).

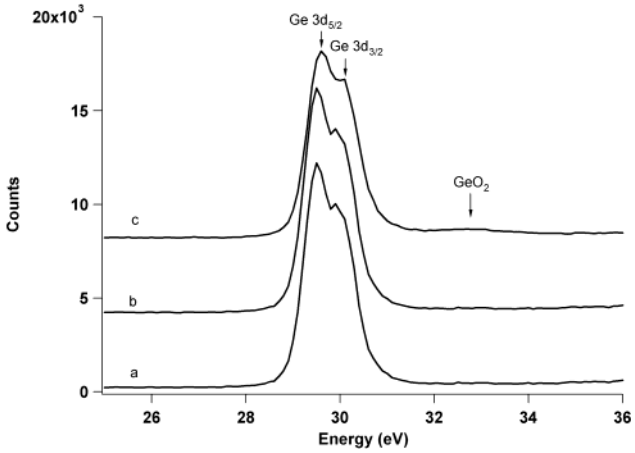

Figure 6. XPS of Ge nanowires in the region of the Ge 3d peaks: (a) immediately after synthesis; (b) after 24 h of atmospheric exposure (3 mol % oxidation of the wires); and (c) 168 h of atmospheric exposure (~7 mol % oxidation). Deconvolution of the Ge and GeO_2 peaks at 29 and 33 eV, respectively, revealed the amount of wire oxidation. The splitting of the Ge signal at 29 eV resolves the $3d_{5/2}$ and $3d_{3/2}$ states.

temperature has been significantly reduced in the nanoscale gold droplets, as recently reported by Wu and Yang,[29] or a nanometer-sized solid nucleation particle can seed wire growth. The latter possibility was recently suggested by Kamins et al.,[30,31] who found that Ti-nucleated Si wires grew at temperatures up to 500 °C below the eutectic, suggesting that a solid nucleation particle has sufficiently high internal diffusion rates to permit wire growth.

While the injection solutions used for all experiments discussed thus far contained 200 mM, complementary experiments with diluted injection solutions at 20 and 800 mM were carried out with TEG and DPG at 450 °C and 13.8 MPa. The results are shown in Figure 7. While the precursor concentration does not appear to affect the morphology of the nanowires grown with DPG, the materials obtained from the TEG experiments show significant concentration dependence. The

(30) Kamins, T. I.; Williams, R. S.; Chen, Y.; Chang, Y. L.; Chang, Y. A. *Appl. Phys. Lett.* **2000**, *76*, 562.
(31) Kamins, T. I.; Williams, R. S.; Basile, D. P.; T., H.; Harris, J. S. *J. Appl. Phys.* **2001**, *89*, 1008.

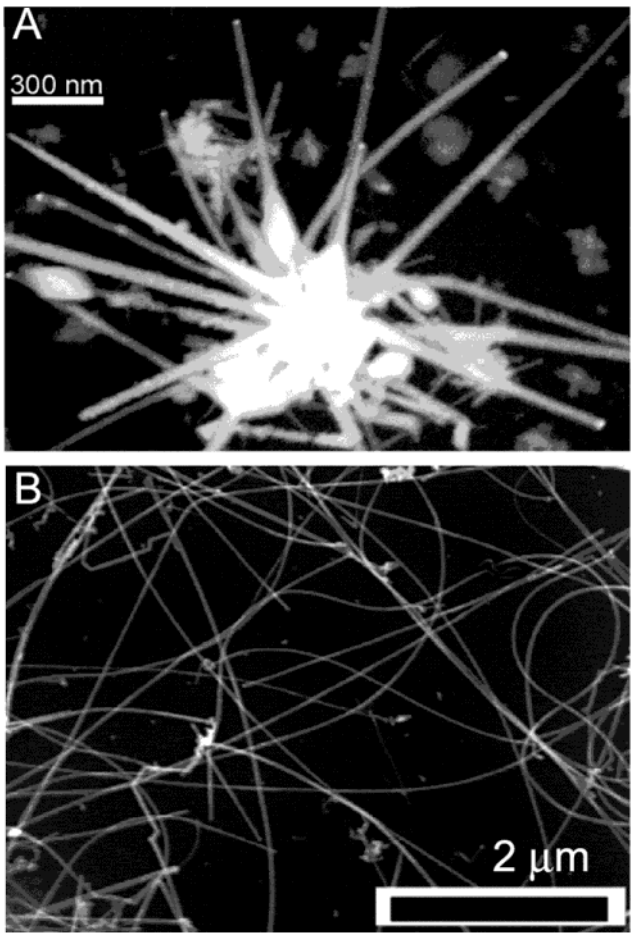

Figure 7. HRSEM images of Ge nanowires grown at different precursor concentrations: (A) image obtained with RBS detector of Ge nanowire structure formed by degrading TEG (20 mM) injected at 450 °C, 13.8 MPa; (B) Ge nanowires formed at 450 °C, 13.8 MPa, with an injection solution of 20 mM DPG. The Au:Ge ratio in both experiments was 1:200. In (A), backscattered electrons show the higher contrast Au particles at some of the tips of the wires protruding from the central structure.

low TEG concentration produces nanowire network structures (Figure 7A) very different from those shown in Figure 2. The "sea urchin" structures seen in Figure 7A contain up to 30 nanowires, with diameters ranging from 20 to 50 nm and lengths up to 1.5 μm. Nanowires grown from DPG at the same concentrations do not exhibit the sea urchin morphology (Figure 7B).

The sea urchin Ge nanowire structures were imaged by HRSEM (Figure 7A) using a Robinson backscattering detector (RBSD). Gold particles exist at many of the tips of the nanowires protruding from the central structure. Zhu and co-workers[32] have reported similar 3D structures composed of amorphous silicon oxide wires radially attached to a Co catalyst particle. The mechanism proposed in ref 32 involves an agglomerated catalyst particle at the core and smaller catalyst particles at the tips of the wires. The "nanoflower" structures observed ref 32 differ in two aspects from our observed structures: (1) EDS measurements did not indicate that Au resides at the center of the structure, and (2) the wires are crystalline, as confirmed by the HRTEM. A possible mechanism for the formation of these structures begins with homogeneous nucleation of a large Ge cluster followed by Au nanocrystal adsorption. The combined effects of low precursor concentration and slower decomposition rate of TEG compared to that of DPG appear to delay Ge wire nucleation for the seed particles. Therefore, increased agglomeration of nonsaturated Au:Ge alloy droplets occurs in the early stage of synthesis compared to the experiments in which the precursor concentration is higher. At later stages in the reaction, Ge continues to add to the agglomerated structure, most likely through dissolution into the Au nanocrystals, which encourage growth of the spikes from the structure.

(32) Zhu, Y. Q.; Hsu, W. K.; Terrones, M.; Grobert, N.; Terrones, H.; Hare, J. P.; Kroto, H. K.; Walton, D. R. M. *Adv. Mater* **1998**, *8*, 1859.

Conclusions

Sterically stabilized gold nanocrystals were used to promote the growth of milligram quantities of Ge nanowires in a supercritical fluid environment. EDS mapping confirmed the significance of Au-nucleating particles to nanowire growth. Nanowire formation was observed at growth temperatures below the eutectic point of the bulk material, possibly due to reduced eutectic temperature in nanostructures or the possibility of a solid nucleation particle. The comparison of DPG and TEG as Ge precursors illustrated the importance of the precursor decomposition rate to the morphology of the synthesized nanowires. The quality of Ge nanowires formed from DPG is superior to that of those obtained from TEG due to the faster decomposition of the former. The optimum temperature range for Ge nanowire synthesis in supercritical cyclohexane is between 350 and 400 °C, while varying the pressure between 13.8 and 38 MPa did not affect the gross wire morphology. Low TEG concentrations favor the formation of aggregated sea urchin nanowire-shaped structures, whereas high concentrations result in the formation of dense nanowire networks for both TEG and DPG. Agglomeration of Au nanocrystals or the Au:Ge droplets during the initial stages of the reactions appears to limit the diameter control of the Ge nanowires nucleated from the Au seeds. The Ge nanowires oxidize to a significant degree upon atmospheric exposure.

Acknowledgment. We thank NSF, the Petroleum Research Fund, and the Welch Foundation for financial support of this work. The authors gratefully acknowledge valuable discussions with L. Pell, K. P. Johnston, and K. Ziegler. We also thank J. P. Zhou and P. Santiago for assistance with the HRTEM.

JA016788I